Sparse-input Detection Algorithm with Applications in Electrocardiography and Ballistocardiography

F. Wadehn[*,1], L. Bruderer[*,1], D. Waltisberg[2], T. Keresztfalvi[1] and H.-A. Loeliger[1]

[1] *Signal and Information Processing Laboratory, ETH Zurich, Gloriastrasse 35, Zurich, Switzerland*
[2] *Institut fuer Elektronik, ETH Zurich, Gloriastrasse 35, Zurich, Switzerland*

Keywords: Ballistocardiography, Heart Rate Estimation, Hypothesis Test, Factor Graphs, System identification, State-space Models, Maximum likelihood, Maximum a posteriori.

Abstract: Sparse-input learning, especially of inputs with some form of periodicity, is of major importance in bio-signal processing, including electrocardiography and ballistocardiography. Ballistocardiography (BCG), the measurement of forces on the body, exerted by heart contraction and subsequent blood ejection, allows non-invasive and non-obstructive monitoring of several key biomarkers such as the respiration rate, the heart rate and the cardiac output. In the following we present an efficient online multi-channel algorithm for estimating single heart beat positions and their approximate strength using a statistical hypothesis test. The algorithm was validated with 10 minutes long ballistocardiographic recordings of 12 healthy subjects, comparing it to synchronized surface ECG measurements. The achieved mean error rate for the heart beat detection excluding movement artifacts was 4.7%.

1 INTRODUCTION

Cardiovascular diseases are among the leading causes of death and severe health impairments both in high-income countries with an aging population, as well as in developing countries, which are increasingly adopting western sedentary lifestyles and diet (Yusuf et al., 2001). Cardiac monitoring appliances range from high resolution devices such as multi-lead ECG or the invasive esophageal ECG (Schnittger et al., 1986) to non-invasive, non-obstructive long time monitoring systems among which pulse oximetry (Yelderman and New Jr, 1983) and ballistocardiography (BCG) (Alihanka et al., 1981) are the most prominent. In ballistocardiography, forces exerted by ventricular blood ejection are measured with force sensors, usually placed below or inside a mattress on which patients are lying. These force measurements can be used to infer heart rates, heart rate variability and even for getting indications about the cardiac output (Cathcart et al., 1953; Inan et al., 2009). BCG signals can be interpreted as an overlap of several oscillations of the body-bed-sensors system. Figure 1 shows a filtered (see Section 3.1) single channel BCG signal and heart-beat times (time of R peak in QRS complex), extracted from a synchronized surface ECG.

---

[*]These two authors contributed equally

Early signal-processing methods for BCG signals (Watanabe et al., 2005; Mack et al., 2009) concerned estimation of heart rates averaged over a few seconds using frequency-based methods. These methods do not provide beat-to-beat resolution or information on irregular arrhythmias. Recently, advanced applications such as heart rate variability analysis or sleep staging, have brought up the challenging task of detecting individual heart beats in a BCG signal. Schemes that rely on a single peak of a, possibly preprocessed, BCG signal lack robustness for most applications due to oscillations caused by one heart beat that decay slowly and overlap with the next heart beat (Bruser et al., 2011).

A variety of methods, proposed for beat-to-beat detection are based on, possibly adaptive, template matching techniques (Shin et al., 2008; Paalasmaa et al., 2014) or sets of features extracted from the BCG signal (Friedrich et al., 2010; Bruser et al., 2011). These approaches have in common that they are not based on a probabilistic framework and their performance, which relies on specific patterns of troughs and peaks, might decrease, if used with stiff systems, where oscillations have not sufficiently decayed and the following impulse might lead to destructive interference. In addition, these algorithms were developed for single-channel measurement sce-
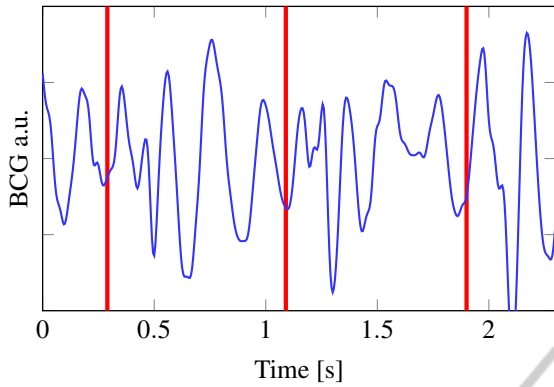
Figure 1: Filtered single channel BCG signal (solid) with heart beat positions (red).

Figure 2: One hearbeat period segment of a measured BCG signal and the estimated state-space model's outputs, obtained with the presented bootstrap system identification approach. Subspace identification with 4-th, 8-th, and 14-th order model resulted in normalized root-mean-squared-error (NRMSE) fits[1] of 32%, 44%, and 52% respectively evaluted on the training data.

narios. Extension of these schemes to process multi-channel measurements, thus taking advantage of more information, is not readily possible. In addition the aforementioned algorithms are tailored to extract instantaneous heart rates from the BCG signals, but do not recover estimates of the relative strength of heart beats.

In this paper, we present a robust heart-beat detection algorithm, which can be used to extract beat-to-beat estimates (e.g., heart rate or the heart rate variability) from ballistocardiogram measurements. By means of an initial training step the method adapts itself to the present BCG data. Individual heartbeat then detects beats in a recursive window-based fashion, using a probabilistic model of the BCG signal. Core of the model is a state-space model representation of the BCG signal and an computationally efficient method for performing hypothesis testing (Reller, 2012). Owing to the explicit modeling of the BCG heart beat pulses our method is thus robust when dealing with beat-to-beat interference in the measurements. Furthermore, the probabilistic treatment allows to quantify the reliability of a potential heart beat detection and is leveraged for removal of small artifacts in the signal. Lastly, the estimation algorithm being based on a maximum likelihood hypothesis-testing procedure, apart from estimates of heart-beat time also infers the relative magnitude of beats. Information on the heart beat's relative magnitude might be useful to get indications on the cardiac output (Kurumaddali et al., 2014).

The paper is structured as follows. At first the BCG signal's is presented along with our algorithm to detect individual heart beats and estimate their magnitude (Section 2). The employed validation dataset and necessary pre-processing are then discussed (Section 3), followed by the results (Section 4).

2 ALGORITHM DESCRIPTION

We model BCG signals as a time-shifted sum of beats. Each beat in turn is modeled as a linear combination of exponentially-decaying oscillations with additive white Gaussian noise. Using linear discrete-time state-space models these signals are described as follows

$$\begin{aligned} X_k &= AX_{k-1} + BU_k \\ Y_k &= CX_k + Z_k, \end{aligned} \quad (1)$$

where the input signal U_k represents the heart beat train, Y_k models the measured BCG signal, and $Z_k \sim \mathcal{N}(0,V)$ is the observation noise. The heart beat train is modeled as a scaled non-uniformly spaced Kronecker comb

$$U_k = \sum_{n=0}^{N} \delta[k - T_n] \cdot \alpha_n, \qquad T_n \in \mathbb{N}, \quad (2)$$

with N heart beats and scaling factors α_n, which serve as indication for the instantaneous cardiac output. The *heart-beat times* T_n and the scaling factors α_n are unknown and estimated from the BCG signal.

The proposed method used to infer the temporal pattern of heart-beats, consists of a model-estimation step, followed by a robust beat-detection algorithm. The purpose of the model-estimation step is to identify a suitable state-space model representation in

---

[1]NRMS is computed as follows

$$\left(1 - \frac{\|\vec{Y} - \hat{\vec{Y}}\|}{\|\vec{Y} - 1/K \sum_{k=1}^{K} Y_k\|} \right) 100\%,$$

where Y and $\hat{Y}$ represent the stacked BCG measurements and predictions of the estimated model.

Algorithm 1: Sparse-input detection.

1: Pre-processing (Section 3.1)
2: 6σ artifact labeling (Section 2.4)
3: Bootstrapped state-space model identification
4: Robust heart-beat detection (Sections 2.2-2.4)
5: Outlier rejection (Section 2.5)

Figure 3: Factor graph of initial part of the BCG signal model.

(1) of the current BCG signal. To this end, sub-space methods were selected, due to their efficiency and their numerical stability (Van Overschee and De Moor, 1996). Subspace methods (e.g., 4SID) are based on the idea that an estimate of the state sequence $\hat{x}$ can be directly estimated from input/output data. Once the state-space sequence is estimated, the system matrices A, B, C are retrieved using a linear least squares fit (Ljung, 1998). The covariance V of the observation noise Z_k can be estimated from data as described in (Van Overschee and De Moor, 1994).

As in our BCG signal model measurements of the input, the heart-beat times and forces, are not available, we use a bootstrap method for approximate system identification: Heart beat excitations are approximated with a signal derived from surface ECG measurements. Specifically, we assume that the ECG signal is given for the first minute of our trial and use the times of the R peaks in the QRS complexes as approximate heart-beat times $\tilde{T}_n$. In addition, $\alpha_n \equiv 1$ is used for all beats in (2). The synchronized BCG measurements, correspond to the outputs Y_k in (1). Currently, our robust beat-detection algorithm is thus tailored for setups where a state-space model representation is known a-priori or setups that allow the use of our suggested bootstrap system identification approach. The input-output system identification is performed using the N4SID algorithm (Van Overschee and De Moor, 1994) with a fixed system order.

Figure 2 demonstrates the approximation of a single-channel BCG signal using a system order of 4, 8, and 14. The task of heart-beat detection, does not require the BCG signal to be perfectly represented by a state-space model: As shown in Section 4, 8-th models, whose fit to the BCG data Figure 2 is clearly inferior to higher order models, can still yield nearly the same error-rate performance for heart-beat detection. Additionally, lower system orders are more robust with respect to variations of the BCG model (1) and demand less computational resources.

2.1 Factor Graph of State-space Model

Since we model the BCG signals probabilistically, our proposed algorithm relies heavily on probabilistic inference methods. These computations can be performed by means of message passing on factor graphs. Factor graphs describe factorizations of multi-variable functions(Kschischang et al., 2001). As shown in (Loeliger et al., 2007), state-space models can also be represented with factor graphs and efficient algorithms for probabilistic inference, such as maximum likelihood estimation and maximum a posteriori estimation can then be derived.
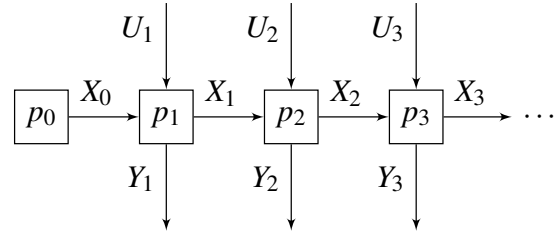
In Forney-style factor-graph (FFG) notation (Kschischang et al., 2001), boxes represent factors, whereas edges represent variables. A node connected to several edges describes a function depending on these variables. As an example, consider the following factorization of the joint probability model for Eq. (1), where a length M BCG signal is observed,

$$p(y_1, \ldots, y_M, x_0, \ldots, x_M | u_1, \ldots, u_M)$$
$$= p(x_0) \cdot \prod_{k=1}^{M} p(y_k, x_k | x_{k-1}, u_k). \qquad (3)$$

The initial part of the FFG that corresponds to this factorization is shown in Fig. 3, where the abbreviation $p_i = p(y_i, x_i | x_{i-1}, u_i)$ was employed.

Each block p_i in Fig. 3 can be expanded to the factor shown in Fig. 4. The proposed algorithms are based on the latter, more detailed, factorization.

Probabilistic inference (e.g., computation of marginal probability densities for maximum a posteriori estimation) is performed by means of message passing. In message passing algorithms, messages μ are exchanged between nodes of the graph. Each node computes output messages based on all incoming messages. Marginal distributions can eventually be obtained from the product of both messages on an edge, which face in opposite direction. Central to the development of our algorithm are forward messages $\overrightarrow{\mu}_{X_k}$ and backward messages $\overleftarrow{\mu}_{X_k}$ for state variables X_k. In particular, these messages represent

$$\overrightarrow{\mu}_{X_k}(x_k) = p(y_1, \ldots, y_{k-1}, x_k | u_1, \ldots, u_k) \qquad (4)$$
$$\overleftarrow{\mu}_{X_k}(x_k) = p(y_k, \ldots, y_N | x_k, u_{k+1}, \ldots, u_N). \qquad (5)$$
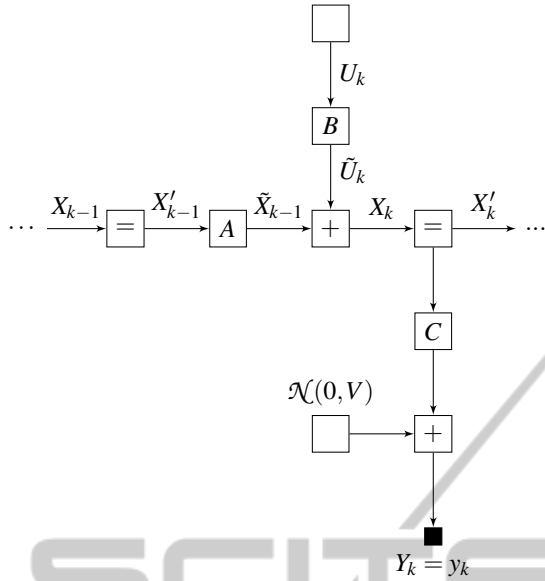
Figure 4: One sample of the FFG of the linear state-space model of BCG measurements.

Consequently, the product of these messages corresponds to the probability density

$$\overrightarrow{\mu}_{X_k}(x_k) \cdot \overleftarrow{\mu}_{X_k}(x_k) = p(y_1, ..., y_N, x_k | u_1, ..., u_N). \quad (6)$$

Given that the current model is a linear function of Gaussian random variables and unknown deterministic variables, inference of edge variables is performed by means of Gaussian message-passing presented in (Loeliger et al., 2007). In this case, messages are Gaussian functionals

$$\overrightarrow{\mu}_X(x) = \mathcal{N}(x | \overrightarrow{m}_X, \overrightarrow{V}_X) \cdot \overrightarrow{\beta}_X. \quad (7)$$

These functionals are fully specified by the mean vector $\overrightarrow{m}$, the covariance matrix $\overrightarrow{V}$, and the scale factor $\overrightarrow{\beta} = \int_{-\infty}^{\infty} \overrightarrow{\mu}(x)dx$. The computation rules for all the nodes present in our FFG model (cf. Fig. 4), are reported in the appendix. For ease of computations, an equivalent dual parametrization is commonly selected for the backward messages $\overleftarrow{\mu}$: The messages are described using the inverse covariance matrix $\overleftarrow{W}$, the weighted mean $\overleftarrow{W} \cdot \overleftarrow{m}$ and the scale factor $\overleftarrow{\gamma} := \overleftarrow{\mu}(0)$.

2.2 Heart-beat Time Estimation

Given a linear state-space model representation in (1) and a sufficiently short multi-channel BCG segment, the goal is to determine the heart-beat time T. The main idea consists in performing a hypothesis test over a time window of N observations and assessing the likelihood that a heart-beat occurred in exactly one

specific position. For each point in time $k \in \{1, ..., N\}$ we have the hypothesis $\mathcal{H}_k$ stating that all inputs in the window, except the k-th are zero.

$$\mathcal{H}_k : U_j = \begin{cases} u_k, & \text{if } j = k \\ 0, & \text{else} \end{cases} \quad (8)$$

To determine the position of the input via maximum likelihood estimation in a hypothesis testing setting, we will compute the likelihood of each hypothesis, which is a function of the corresponding input magnitude

$$\begin{aligned} \mathcal{L}_k(u_k) &= p(y | \mathcal{H}_k, u_k) \\ &= p(y | U_1 = 0, ..., U_k = u_k, ..., U_N = 0) \quad (9) \\ &= \overleftarrow{\mu}_{U_k}(u_k) \end{aligned}$$

We thus get the likelihood vector $\vec{L}(\vec{u})$ with:

$$\vec{L}(\vec{u}) = (\mathcal{L}_1(u_1), ..., \mathcal{L}_N(u_N))^\mathsf{T} \quad (10)$$

Since $\vec{L}$ is a vector valued function, we will integrate out each input u_k assuming a flat prior over the real or positive real numbers[2] to reduce the likelihood functions for each hypothesis to a single value.

$$\bar{\mathcal{L}}_k = \int_0^\infty \overleftarrow{\mu}_{U_k}(u_k) du_k = 0.5 \cdot \overleftarrow{\beta}_{U_k} \cdot \text{erfc} \left(-\frac{\overleftarrow{m}_{U_k}}{\sqrt{2\overleftarrow{V}_{U_k}}} \right) \quad (11)$$

To determine the beat position $\hat{T}$, we select the index of the most likely hypothesis

$$\hat{T} = \underset{k}{\text{argmax}} \ \bar{\mathcal{L}}_k. \quad (12)$$

The rationale behind this hypothesis test is to compare how well the signal preceding the assumed input is described by the state-space model in the absence of an input and how well the oscillations following the assumed input, fit to the model's response to an input. The robustness of this estimation procedure is increased if the real heart beat is not too close to the window's borders. Estimation of the input magnitude is done by means of maximum-a-posteriori estimation using the posterior distribution of u_k. The posterior distribution, is computed taking a flat prior $p(u_k)$ as in (11) and is proportional (i.e., a proportionality factor independent of u_k) to

$$p(u_k | \mathcal{H}_k, y) = \overleftarrow{\mu}_{U_k}(u_k). \quad (13)$$

---

[2]For the final algorithm we integrated over the positive real numbers, which reflects the hypothesis that heart beats are a positive impulses. This assumption leads to likelihoods with less side peaks and thus to a more robust beat detection

Consider the factor graph in Fig. 4 with hidden states $x = (x_0, \ldots, x_N)$ and where each variable U_k is set to 0, thus expressing the probability density

$$p(y, x | U_1 = 0, \ldots, U_N = 0). \tag{14}$$

To detect the heart beat time index, messages $\overleftarrow{\mu}_{U_k}(u_k)$ for all possible k are computed in one foward sweep and one backward sweep. It now follows that the backward message $\overleftarrow{\mu}_{U_k}(u_k)$ expresses

$$\overleftarrow{\mu}_{U_k}(u_k) = p(y | U_1 = 0, \ldots, U_k = u_k, \ldots, U_N = 0), \tag{15}$$

and using (11), with a flat prior on positive input amplitudes, the heart beat estimate $\hat{T}$ can be computed from (12), as well as the input magnitude

$$u_k^{MAP} = \begin{cases} \overleftarrow{m}_{U_k}, & \overleftarrow{m}_{U_k} \geq 0 \\ 0, & \overleftarrow{m}_{U_k} < 0 \end{cases}. \tag{16}$$

Note that computational complexity of this heart beat time estimation is $O(N)$, thus linear in the length of the window.

2.3 Window-based Adaptive Beat Detection

Having established an algorithm to estimate both the input position and its magnitude given a time window containing one heart beat, the question that remains is how to choose the windows properly to cover the whole signal. Our approach was to use an adaptive jumping window procedure. The bootstrapping begins with a large window e.g. 2s such that it contains at least one heart beat with high probability. The estimated position of that heart beat is denoted as $\hat{T}_1$. Given an estimated heart beat position $\hat{T}_k$, place a symmetric window around the position where the next beat is assumed to be, denoted as M_{k+1}. Defining an average *heart beat period* as $HBP_k = (\hat{T}_k - \hat{T}_{k-d})/d$, with $d = 3$ or $d = 5$ having proved to yield good results[3], and assuming an initial *HBP* of 1 s, we get

$$M_k = \hat{T}_{k-1} + HPB_{k-1}$$
$$W_k = [M_k - \lfloor HBP_{k-1}/2 \rfloor, M_k + \lfloor HBP_{k-1}/2 \rfloor].$$

2.4 Automatic Artifact Detection

Movement artifacts can severely impair BCG measurements and extraction of heart-beat times becomes impossible. Initial system identification and reliable estimation of heart-beat times both require that corrupted signal segments are detected automatically. To

---

[3]For the final implementation $d = 3$ was chosen
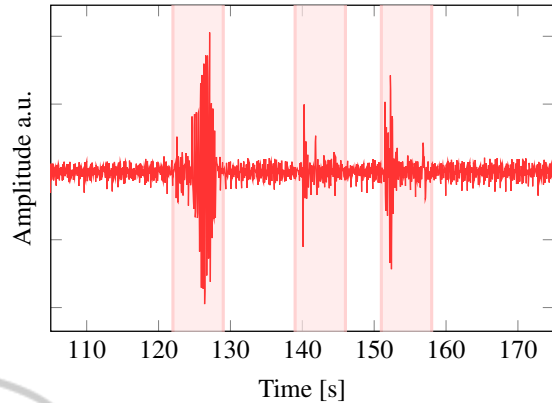
Figure 5: Prominent artifacts in the BCG signal, are labeled (shaded) by the 6σ method.

this end, we devise a two-level approach. At first, strong movement artifacts, which are characterized by a much higher amplitude, are removed after pre-processing of the measurements. This automatic detection step, labels parts of the signal outside the 6-sigma band[4] as artifacts. In a further step, short intervals ($< 0.5\,s$) between two adjacent labeled 6-sigma bands, were also removed. In this way the BCG signal is partitioned into useful signal intervals and movements artifacts, which do not contain information about the heart beats as can be seen in Figure 5.

The aforementioned labeling algorithm works well, when movement artifacts are strong and have a short duration (e.g. leg movements). In contrast, a constant presence of small movement artifacts (e.g. caused by tremor), would result in a very small variance of the signal and the movement-artifact detection algorithm would exclude parts of the signal with slightly elevated amplitude from which the heart beats could possibly still be extracted. For such signals, we take advantage of the probabilistic modeling framework: If a corrupted BCG segment is observed and the model is not able to explain the data well, a significant drop in the computed likelihood is observed. The second level of our automatic artifact detection method thus drops estimates $\hat{T}$ if the average likelihood of the window drops below 50% the prior short-time average likelihood values. Instead, the estimated heart-beat time is predicted from past measurements as

$$\hat{T}_k = \hat{T}_{k-1} + HPB_{k-1}.$$

In Figure 6, false estimates are observed from second 124 until second 126 caused by a small artifact, which was not recognized by the 6σ method. However, the corresponding segment clearly exhibits a sig-

---

[4]The 6-sigma band is defined as the amplitude values falling in the interval of $\pm 6\sigma + \mu$
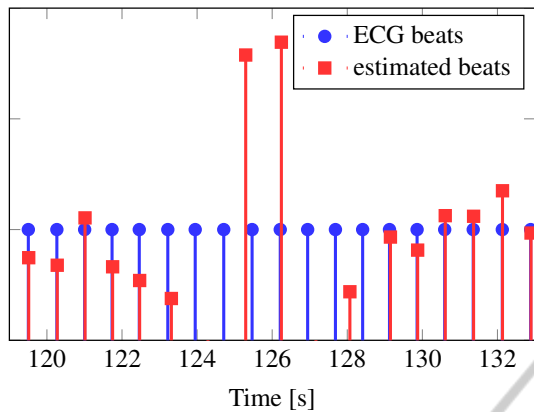
Figure 6: Heart beat detection and input magnitude estimation. Having no information about the instantaneous cardiac output from the ECG data, we plot the heart beat magnitude (black) as a uniform Dirac comb. Movement artifacts at 124s-126s cause midsections, which can be detected from drops in the likelihood as shown in Figure 7

nificant drop in the average likelihood as shown in Figure 7.

2.5 Post-processing

Following the recommendations of (Friedrich et al., 2010), we assume a maximum average heart rate[5] of 120 BPM and a minimum heart rate of 30 BPM. Considering that heart rate measurements are supposed to occur during rest these bounds are appropriate. These averaging durations are in accordance with (Bruser et al., 2011), which states that cardiac monitoring devices can have an update time of up to 10s following the recommendations of ANSI/AAMI/ISO EC13.

3 MATERIALS AND METHODS

To validate our heart-beat detection method we used a dataset containing ECG measurements and two-channel BCG measurements. The dataset comprises 12 healthy subjects (10 male, 2 female) in the age range of 23-32 years. BCG signals were recorded for 10 minutes in supine position (facing up), using piezoelectric pressure sensors placed below the mattress in the area where the torso was assumed to be. Consequently, torso-ventral displacements, as defined in (Scarborough et al., 1956), were measured. For validation purposes, a three lead surface ECG synchronized to the BCG signal was recorded. Instantaneous heart rates ranged from 33 BPM and up to 88 BPM across all 12 subjects.

---

[5]The average heart rate is computed by taking the average over 5 consecutive beats.
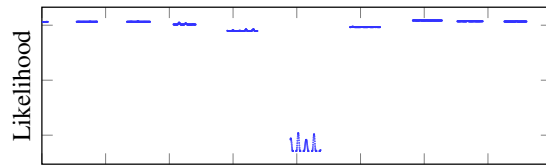
Figure 7: Movement artifacts are detected by drops in likelihood values. The corrupted signal is recognized and corrected assuming a constant average heart rate. This refinement increases stability and reduces the average heart beat detection error rate.
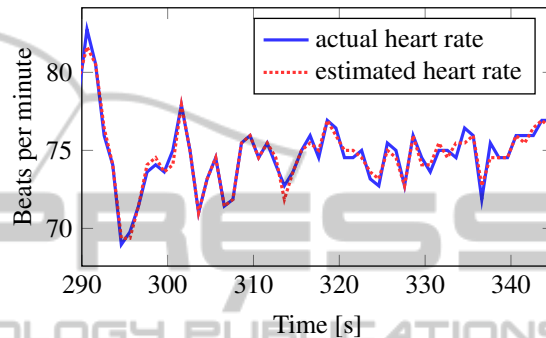
Figure 8: Real ECG-based instantaneous heart rate compared to the instantaneous heart rate extracted from the estimated heart-beat times of our method.

3.1 Pre-processing of BCG and ECG Measurements

Prior to our algorithm, the BCG signal was decimated[6] from 1000 Hz to 200 Hz primarily to reduce computational costs and also noise. A 10-th order, zero-phase bandpass filter (0.5Hz-30Hz) was combined with a second-order IIR notch filter at 50 Hz, using the DSP System toolbox in MATLAB 2014a, to remove respiratory movements and to remove strong electrical disturbances at 50 Hz. The ECG signal was high-pass filtered with a 5-th order Butterworth filter at 2 Hz cut-off to remove baseline wandering. Heart beats were then extracted via peak detection from the filtered ECG signal.

4 PERFORMANCE EVALUATION

The proposed beat-to-beat estimation algorithm was validated using ECG measurements as ground truth in the following way: The ECG heart beat train, containing M heart beats, was split into M segments. The segments are chosen such that each one contains exactly one heart-beat and their union covers the whole ECG signal. Given heart beats at times T_{k-1}, T_k and

---

[6]Downsampling and anti-alias filtering

T_{k+1}, the k-th segment s_k is defined as

$$s_k = [T_k - \lfloor (T_k - T_{k-1})/2 \rfloor, T_k + \lfloor (T_{k+1} - T_k)/2 \rfloor].$$

The estimate $\hat{T}_k$ is counted as correct, if exactly one beat was detected and $\hat{T}_k \in [T_k - 25\,\text{ms}, T_k + 25\,\text{ms}]$. Note that the duration between the electrical activation and the actual blood ejection displays a variation of around 8 ms (Friedrich et al., 2010) and thus, is the maximum precision a beat localization using BCG measurements can achieve. Assuming an average window length of 1 s, corresponding to 60 BPM, the $\hat{T}_k$ is required to have a precision of $\pm 2.5\%$.

Figure 9 shows the heart beat detection error rate as a function of even system orders[7] of the state space model used to describe the BCG signal of subject A. We can see that too low system orders are not suited for modeling the BCG signal and lead to very high error rates. Two channel measurements outperform single channel measurements for almost all system orders except for very low system orders (2 and 4), for which it is better to use single channel measurements, due to the lower complexity of the model required to describe the single channel measurements. The increasing error rate with system order above 20 could be hinting to overfitting, when system orders are too high. On the other hand it is also possible that numerical precision issue arise when performing message passing in factor graphs of state space models of such high order.

The error-rate performance of the presented method is evaluated with two 10 minutes long ballistocardiogram recordings of 12 healthy subjects, excluding sections of the signal containing movement artifacts, which do not provide information about the heart-beat times. The resulting error rate, averaged over the test subjects, is 4.7% with a standard error of the mean of 2.8%. A 14-th order state-space representation is used to describe the BCG signal. These performance metrics include one outlier subject, whose BCG signal contains multiple movement artifacts, leading to an error rate of 35%. Excluding the outlier, the mean error rate decreases to 3.4% with a standard error of the mean of 1.3%.

Automatic artifact detection on the present dataset results in an average estimation coverage for each channel, thus the percentage of the signal or windows not detected as corrupted by movement artifacts. After the first 6σ labeling method the average coverage is 95%. Subsequent detection using the likelihood-based method (see Section 2.4), additionally drops 5% of the windows. Therefore reducing average coverage to around 90%.

---

[7]Even system orders describe the output signal solely as a linear combination of exponentially decaying oscillations
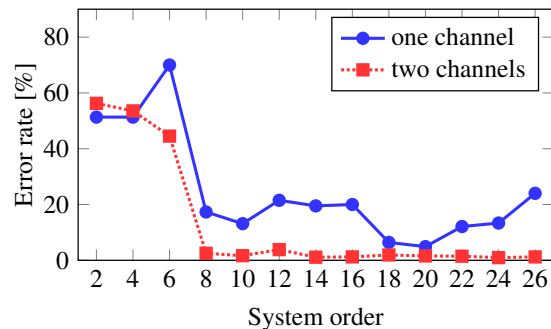
Figure 9: Heart beat detection error rate for subject A as a function of the system order for single and two-channel measurements.

Figure 8 compares the beat-to-beat (instantaneous) heart rate extracted from ECG and from the estimates $\hat{T}$ of the suggested method. The estimated heart-beat times reveal even small fluctuations in the beat-to-beat times. The average interval error between actual heart beats (ECG) and estimated heart beats was computed according to (Friedrich et al., 2010) resulting in an average heart beat interval error of 33.1 ms. Note that the average heart beat detection error rate, introduced above, is better suited to assess our algorithm, as it identifies single heart beats (i.e., beat detection and time $\hat{T}_k$) and not the intervals between heart beats.

The heart beat detection algorithm takes around 60 s to estimate instantaneous heart rates in a 10 minutes long two-channel BCG signal using MATLAB R2014a on a 3.33 GHz, 8 GB personal computer, including system estimation, loading of data and preprocessing. The pure heart beat estimation takes around 35 s, for the 10 minutes long BCG sequences, thus when allowing a small delay (e.g. 5 s) and a start up-time for 30 s the algorithm could run in real time, especially when implemented in faster programming languages such as C/C++.

5 DISCUSSION AND CONCLUSIONS

We have presented a novel method to extract beat-to-beat data from ballistocardiograms. Given an estimated or known linear state-space model representation of the ballistocardiogram signal, heart beats are extracted from measured data using a robust input-estimation algorithm. We have shown that additional measurement channels (i.e., multiple sensors) yield significant performance improvements in terms of error-rate and robustness. Owing to the model-based approach, the method can correctly extract movement

artifacts from measured data and recognize when beat detection is impaired or not possible. Validation of the method on ballistocardiogram measurements of 12 healthy subjects showed 4.7% average beat-detection error rate. The presented algorithm lends itself to application on a multitude of almost periodic signals, especially in cardiology.

Currently, the algorithm at first adapts itself to a specific BCG signal, as described in Section 2. It is likely that alterations of the system (e.g., changed body position) will trigger the likelihood-based artifact detection routine (see Section 2) and a new system identification step will become necessary. However, in the present dataset, subjects were laying still and this issue was not observed.

A further complication, which was also not observed in the current dataset, may arise when strong heart-rate variability occurs. The window-based approach may either select a window where no beat is present or a window with two beats. In the first case, a false-positive beat will be detected, while in the other case, the algorithm will miss a beat and make a false-negative error. This issue could be addressed by considering the relative likelihood value of a beat estimate to the other indices with large likelihood values and deciding if two beats are present or none. Also schemes which run the window-based detection schemes multiple times and each time including the currently detected beats and models on heart-rate variability might mitigate these type of errors.

Blind system identification i.e., estimation of the state-space model solely on BCG measurements, would facilitate applicability of the current method. As a consequence, the resulting method would not require ECG measurement equipment and would be able to adapt to varying external factors (e.g., sleeping position). Moreover, investigating on the relation between the estimated input magnitude and the instantaneous cardiac output, which is a key biomarker for various cardiovascular diseases, seems to be a promising direction for future research.

A further enhancement can be achieved by multiplying the hypothesis likelihood with a Gaussian window, centered around the assumed input, serving as a prior on the heart beat position. This refinement significantly improves error rates, when the BCG signal is hardly contaminated by movement artifacts. On the other hand when the signal contains several movement artifacts, it is better not to assume any prior on the beat position to avoid error propagation. To deal with a general BCG signal, possibly heavily contaminated with artifacts, the Gaussian window was omitted in the performance evaluation in subsection 4.

Table 1: Performance metrics.

Metric	Unit	Value
Signal duration	min	10
Coverage 6-σ labeling	%	95
Coverage likelihood drop labeling	%	90
HB detection error rate	%	4.7
HB interval error	ms	33.1

ACKNOWLEDGEMENTS

REFERENCES

Alihanka, J., Vaahtoranta, K., and Saarikivi, I. (1981). A new method for long-term monitoring of the ballistocardiogram, heart rate, and respiration. *Am J Physiol*, 240(5):R384–92.

Bruser, C., Stadlthanner, K., de Waele, S., and Leonhardt, S. (2011). Adaptive beat-to-beat heart rate estimation in ballistocardiograms. *IEEE Transactions on Information Technology in Biomedicine,*, 15(5):778–786.

Cathcart, R. T., Field, W. W., and Richards Jr, D. W. (1953). Comparison of cardiac output determined by the ballistocardiograph (nickerson apparatus) and by the direct fick method. *Journal of Clinical Investigation*, 32(1):5.

Friedrich, D., Aubert, X., Fuhr, H., and Brauers, A. (2010). Heart rate estimation on a beat-to-beat basis via ballistocardiography-a hybrid approach. In *Engineering in Medicine and Biology Society (EMBC), 2010 Annual International Conference of the IEEE*, pages 4048–4051. IEEE.

Inan, O., Etemadi, M., Paloma, A., Giovangrandi, L., and Kovacs, G. (2009). Non-invasive cardiac output trending during exercise recovery on a bathroom-scale-based ballistocardiograph. *Physiological measurement*, 30(3):261.

Kschischang, F. R., Frey, B. J., and Loeliger, H.-A. (2001). Factor graphs and the sum-product algorithm. *Information Theory, IEEE Transactions on*, 47(2):498–519.

Kurumaddali, B., Marimuthu, G., Venkatesh, S. M., Suresh, R., Syam, B., and Suresh, V. (2014). Cardiac output measurement using ballistocardiogram. In *The 15th International Conference on Biomedical Engineering*, pages 861–864. Springer.

Ljung, L. (1998). *System identification*. Springer.

Loeliger, H.-A., Dauwels, J., Hu, J., Korl, S., Ping, L., and Kschischang, F. R. (2007). The factor graph approach

to model-based signal processing. *Proceedings of the IEEE*, 95(6):1295–1322.

Mack, D. C., Patrie, J. T., Suratt, P. M., Felder, R. A., and Alwan, M. (2009). Development and preliminary validation of heart rate and breathing rate detection using a passive, ballistocardiography-based sleep monitoring system. *Information Technology in Biomedicine, IEEE Transactions on*, 13(1):111–120.

Paalasmaa, J., Toivonen, H., and Partinen, M. (2014). Adaptive heartbeat modelling for beat-to-beat heart rate measurement in ballistocardiograms. *IEEE Journal of Biomedical and Health Informatics,*, PP(99):1–1.

Reller, C. (2012). *State-space methods in statistical signal processing: New ideas and applications*. PhD thesis, ETH Zurich.

Scarborough, W. R., Talbot, S. A., Braunstein, J. R., Rappaport, M. B., Dock, W., Hamilton, W., Smith, J. E., Nickerson, J. L., and Starr, I. (1956). Proposals for ballistocardiographic nomenclature and conventions: revised and extended report of committee on ballistocardiographic terminology. *Circulation*, 14(3):435–450.

Schnittger, I., Rodriguez, I. M., and Winkle, R. A. (1986). Esophageal electrocardiography: a new technology revives an old technique. *The American journal of cardiology*, 57(8):604–607.

Shin, J., Choi, B., Lim, Y., Jeong, D., and Park, K. (2008). Automatic ballistocardiogram (bcg) beat detection using a template matching approach. In *Engineering in Medicine and Biology Society, 2008. EMBS 2008. 30th Annual International Conference of the IEEE*, pages 1144–1146.

Van Overschee, P. and De Moor, B. (1994). N4sid: Subspace algorithms for the identification of combined deterministic-stochastic systems. *Automatica*, 30(1):75–93.

Van Overschee, P. and De Moor, B. (1996). Subspace identification for linear systems: Theory, implementation. *Methods*.

Watanabe, K., Watanabe, T., Watanabe, H., Ando, H., Ishikawa, T., and Kobayashi, K. (2005). Noninvasive measurement of heartbeat, respiration, snoring and body movements of a subject in bed via a pneumatic method. *Biomedical Engineering, IEEE Transactions on*, 52(12):2100–2107.

Yelderman, M. and New Jr, W. (1983). Evaluation of pulse oximetry. *Anesthesiology*, 59(4):349–351.

Yusuf, S., Reddy, S., Ôunpuu, S., and Anand, S. (2001). Global burden of cardiovascular diseases part i: general considerations, the epidemiologic transition, risk factors, and impact of urbanization. *Circulation*, 104(22):2746–2753.

APPENDIX

Message Passing

Measurements are plugged into the factor graph, resulting in Dirac delta messages. Let $X_k \in \mathbb{R}^n$ and $Y_k \in \mathbb{R}^p$

$$\overleftarrow{m}_{Y_k} = y_k$$
$$\overleftarrow{V}_{Y_k} = 0$$
$$\overleftarrow{\beta}_{Y_k} = 1$$
$$\overleftarrow{\mu}_{Y_k}(y_k) = \delta(y_k - y_k^{obs})$$

Sum-product message passing through the sum-factor $(\tilde{Y}_k + Z_k)$.

$$\overleftarrow{W}_{\tilde{Y}_k} = V^{-1}$$
$$\overleftarrow{W}_{\tilde{Y}_k}\overleftarrow{m}_{\tilde{Y}_k} = V^{-1}y_k$$
$$\overleftarrow{\beta}_{\tilde{Y}_k} = \overleftarrow{\beta}_{Y_k} \cdot \overrightarrow{\beta}_{Z_k} = 1$$

$$\overleftarrow{\mu}_{\tilde{Y}_k}(\tilde{y}_k) = (2\pi)^{-\frac{p}{2}}\det(V)^{-\frac{1}{2}}e^{-\frac{1}{2}(\tilde{y}_k - y_k)^{\mathsf{T}}V^{-1}(\tilde{y}_k - y_k)}$$
$$\overleftarrow{\mu}_{\tilde{Y}_k}(0) = \overleftarrow{\gamma}_{\tilde{Y}_k} = (2\pi)^{-\frac{p}{2}}\det(V)^{-\frac{1}{2}}e^{-\frac{1}{2}y_k^{\mathsf{T}}V^{-1}y_k}$$

$$\overleftarrow{W}_{X_k''} = C'\overleftarrow{W}_{\tilde{Y}}C$$
$$\overleftarrow{W}_{X_k''}\overleftarrow{m}_{X_k''} = C'\overleftarrow{W}_{\tilde{Y}_k}\overleftarrow{m}_{\tilde{Y}_k}$$
$$\overleftarrow{\gamma}_{X_k''} = \overleftarrow{\gamma}_{\tilde{Y}_k}$$

Forward Message Passing

Forward message passing corresponds to Kalman filtering in the state space model. The update equations are

$$m_{X_k'} = \overrightarrow{m}_{X_k} + \overrightarrow{V}_{X_k}C^{\mathsf{T}}G(\overleftarrow{m}_{\tilde{Y}_k} - C\overrightarrow{m}_{X_k})$$
$$\overrightarrow{V}_{X_k'} = \overrightarrow{V}_{X_k} - \overrightarrow{V}_{X_k}C^{\mathsf{T}}GC\overrightarrow{V}_{X_k}$$
$$G^{-1} = \overleftarrow{V}_{\tilde{Y}_k} + C\overrightarrow{V}_{X_k}C^{\mathsf{T}}$$

$$V: = \overleftarrow{V}_{\tilde{Y}_k} + C\overrightarrow{V}_{X_k}C^{\mathsf{T}}$$
$$m: = C\overrightarrow{m}_{X_k} + \overleftarrow{m}_{\tilde{Y}_k}$$
$$\overrightarrow{\beta}_{X_k'} = \overrightarrow{\beta}_{X_k}\overleftarrow{\beta}_{\tilde{Y}_k}\sqrt{\frac{1}{(2\pi)^p \cdot \det(V)}}e^{-\frac{m^{\mathsf{T}}V^{-1}m}{2}}$$

$$\overrightarrow{m}_{\tilde{X}_k} = A\overrightarrow{m}_{X_k'}$$
$$\overrightarrow{V}_{\tilde{X}_k} = A\overrightarrow{V}_{X_k'}A^{\mathsf{T}}$$
$$\overrightarrow{\beta}_{\tilde{X}_k} = \overrightarrow{\beta}_{X_k'}$$

$$\overrightarrow{m}_{X_{k+1}} = \overrightarrow{m}_{\tilde{X}_k}$$
$$\overrightarrow{V}_{X_{k+1}} = \overrightarrow{V}_{\tilde{X}_k}$$
$$\overrightarrow{\beta}_{X_{k+1}} = \overrightarrow{\beta}_{\tilde{X}_k}$$

Backward Message Passing

Backward message passing corresponds to Kalman smoothing in the state space model. The update equations are

$$\overleftarrow{W}_{X_k} = \overleftarrow{W}_{X_k''} + \overleftarrow{W}_{X_k'}$$
$$\overleftarrow{W}_{X_k} \overleftarrow{m}_{X_k} = \overleftarrow{W}_{X_k''} \overleftarrow{m}_{X_k''} + \overleftarrow{W}_{X_k'} \overleftarrow{m}_{X_k'}$$
$$\overleftarrow{\gamma}_{X_k} = \overleftarrow{\gamma}_{X_k'} \overleftarrow{\gamma}_{X_k''}$$
$$\overleftarrow{\beta}_{X_k} = \overleftarrow{\gamma}_{X_k} \sqrt{\frac{(2\pi)^n}{\det(\overleftarrow{W}_{X_k})}} e^{\overleftarrow{m}_{X_k} \overleftarrow{W}_{X_k} \overleftarrow{m}_{X_k}/2}$$

$$\overleftarrow{W}_{X_k'} = A^{\mathsf{T}} \overleftarrow{W}_{\tilde{X}_k} A$$
$$\overleftarrow{W}_{X_k'} \overleftarrow{m}_{X_k'} = A^{\mathsf{T}} \overleftarrow{W}_{\tilde{X}_k} \overleftarrow{m}_{\tilde{X}_k}$$
$$\overleftarrow{\gamma}_{X_k'} = \overleftarrow{\gamma}_{\tilde{X}_k}$$

Rejoining Messages

To determine the marginal distribution of U_k we combine the forward and backward messages.

$$\overleftarrow{m}_{\tilde{U}_{k+1}} = \overleftarrow{m}_{X_{k+1}} - \overrightarrow{m}_{\tilde{X}_k}$$
$$\overleftarrow{V}_{\tilde{U}_{k+1}} = \overleftarrow{V}_{X_{k+1}} + \overrightarrow{V}_{\tilde{X}_k}$$
$$\overleftarrow{\beta}_{\tilde{U}_{k+1}} = \overrightarrow{\beta}_{\tilde{X}_k} \overleftarrow{\beta}_{X_{k+1}}$$

For the heart beat estimation problem we assume that the input is scalar.

$$\overleftarrow{W}_{U_k} = B^{\mathsf{T}} \overleftarrow{W}_{\tilde{U}_k} B$$
$$\overleftarrow{W}_{U_k} \overleftarrow{m}_{U_k} = B^{\mathsf{T}} \overleftarrow{W}_{\tilde{U}_k} \overleftarrow{m}_{\tilde{U}_k}$$

$$\overleftarrow{\beta}_{U_k} = \overleftarrow{\beta}_{\tilde{U}_k} \sqrt{\frac{1}{(2\pi)^{n-1}}} \sqrt{\frac{\det(\overleftarrow{V}_{U_k})}{\det(\overleftarrow{V}_{\tilde{U}_k})}} e^{-\overleftarrow{m}_{\tilde{U}_k}^{\mathsf{T}} \overleftarrow{W}_{\tilde{U}_k} V \overleftarrow{W}_{\tilde{U}_k} \overleftarrow{m}_{\tilde{U}_k}/2}$$
$$V: = \overleftarrow{V}_{\tilde{U}_k} - B \overleftarrow{V}_{U_k} B^{\mathsf{T}}$$